Density Dependence of ^{129}Xe Chemical Shifts in Mixtures of Xenon and Other Gases*

A. KEITH JAMESON
Department of Chemistry, Loyola University, Chicago, Illinois 60626
AND
CYNTHIA J. JAMESON
Department of Chemistry, University of Illinois at Chicago Circle, Chicago, Illinois 60680
AND
H. S. GUTOWSKY
Noyes Chemical Laboratory, University of Illinois, Urbana, Illinois 61801

(Received 29 April 1970)

Unlike other chemical shifts in gaseous systems which have been found to have strictly linear dependence on density, we have found the ^{129}Xe chemical shift in pure xenon gas to have a quadratic and cubic dependence in addition to the dominant linear dependence on density. This implies the importance of three or more body interactions in xenon. In mixtures of xenon with another gas (Ar, Kr, CO_2, HCl, CH_4, CH_3F, CH_2F_2, CHF_3, CF_4), the dependence of the ^{129}Xe chemical shift on the density of the other gas is found to be linear within experimental error, and varying from 2300–11 700 ppm/mol cc^{-1}. These shifts are orders of magnitude greater than the reported H and F shifts in gases. Analysis of the results show that the density dependence cannot adequately be reproduced by the contributions, $\sigma_1=\sigma_b-B\langle\epsilon^2\rangle-B\langle F^2\rangle$, which had been adequate for H and F shifts. The general formulation for calculation of the A and B parameters, the coefficients of the linear and quadratic electric field terms in the theory of chemical shift in gases, is developed. An approximate calculation of B for atoms is given, and the repulsive and anisotropic contributions are estimated. The sensitivity of the chemical shift to the form of the intermolecular potential is suggested in the case of Xe and the fluoromethanes where the results are consistent with a noncentral field potential but not with a central field potential like the Lennard-Jones.

INTRODUCTION

There is current interest in the effect of intermolecular interactions on NMR chemical shifts[1,2] and coupling constants.[2] Solvent effects, hydrogen bonding shifts, and ionic shifts among others have been attributed to intermolecular interactions.

Interpretation of gas-phase chemical shifts would seem to be more accessible than interpretation of either liquid or solid-state data. Solid-state measurements are usually subject to the experimental problem of low resolution due to line broadening by neighbor nuclei. Although high resolution is attainable in liquids, the liquid state is poorly understood theoretically. On the other hand, the gas phase is more amenable to theoretical interpretation, and resolution of gas-phase spectra is unhampered by dipolar broadening.

Chemical-shift measurements in mixed gases hold great promise in being a useful tool in measuring directly the interaction between unlike molecules. X–Y interaction potentials have usually been determined from measurements of transport properties and virial coefficients of mixtures of X and Y. The properties which are measured are averages over the X–X, Y–Y, and X–Y interactions, and there is no way of adjusting the X and Y concentrations to make the X–Y interactions dominant. What is usually done is to subtract the effects of the X–X and Y–Y interactions from the measured property. On the other hand, with the NMR chemical shift one can measure X–Y interactions directly, since one sees only X–X and X–Y interactions with this tool. It is possible to reduce the X concentration sufficiently (limited by signal-to-noise ratio) such that one sees predominantly X–Y interactions. Furthermore, NMR gives us the unique advantage of seeing the interaction of a pair of molecules from the point of view of each one of them, as well as from the point of view of different parts of one or both. For example, in NMR measurements on a mixture of CHF_3 and Xe, the ^{129}Xe chemical shift will show the effect of Xe–CHF_3 interactions on Xe while the ^{19}F and ^1H chemical shifts will show the effect of Xe–CHF_3 interactions at the fluorine and hydrogen positions of the CHF_3 molecule. The ultimate goal would be the extraction of intermolecular potentials from NMR data, after the nature of the dependence of the NMR parameters on the intermolecular potential has been established.

The ^1H and ^{19}F NMR studies which have been conducted on gaseous systems[2] show that chemical shift is linearly dependent on density. That is, in the virial expansion of shielding in descending powers of molar volume (in ascending powers of density), $\sigma=\sigma_0+\sigma_1\rho+\sigma_2\rho^2+\cdots$, only the linear density term need be included. This implies that the interactions which are important are binary. σ_1 is measured as the slope of a plot of chemical shift vs density. The density dependence was interpreted in terms of the following contributions[2]:

$$\sigma_1=\sigma_b+\sigma_W+\sigma_\epsilon+\sigma_a+\sigma_{\text{rep}}. \quad (1)$$

The anisotropy contribution σ_a was found to be negligibly small. The polar, σ_ϵ, and van der Waals, σ_W, terms were interpreted as $\sigma_\epsilon=-A\langle\epsilon_z\rangle-B\langle\epsilon^2\rangle$ and $\sigma_W=-B\langle F^2\rangle$. The averages, $\langle\epsilon_z\rangle$, $\langle\epsilon^2\rangle$, and $\langle F^2\rangle$, were calculated using a Stockmayer potential (central field

Lennard-Jones potential plus electrical dipoles). A and B are parameters obtained by "best fitting" the experimental density dependence of the shifts. The repulsive term, σ_{rep}, was neglected. This interpretation was found to be quite successful for ^{1}H, in which σ_1 is dominated by $\sigma_b - A\langle\epsilon_z\rangle$, and for ^{19}F, in which σ_1 is dominated by $\sigma_\epsilon + \sigma_W$.

Although the experimental NMR data on ^{1}H and ^{19}F have been adequately interpreted in these terms, the reverse process of extraction of information about interaction potentials from these data is another matter. The nonpolar, Lennard-Jones part of these potentials was obtained by using combining rules: The intermolecular potential between X and Y molecules is approximated by a combination of parameters of the X–X interaction potential and the Y–Y interaction potential. The parameters A and B are "best-fit" parameters which probably absorb much of the information we want. The collisions are still approximated to be isotropic, somewhat like collisions of spheres with certain electrical dipolar properties. The effect of nonisotropy of collisions, if any, may have been absorbed in the A and B parameters. The inadequacy of the combining rules used for the unlike-gas potentials may likewise have been absorbed in A and B. Since σ_{rep} was not included, the adequacy of the repulsive part of the potential cannot be determined. The small molecules studied were still fairly complicated ones for which the measurements of transport properties and such are not as extensive as for the rare gases.

To eliminate some of the above difficulties, we decided to use Xe as the probe molecule. Xenon is an ideal probe molecule. Its advantages are many: The molecule has no structure or electrical moments; being a monatomic molecule, any changes in the electronic distribution are transmitted directly to the Xe nucleus. The ^{129}Xe isotope to be studied has no nuclear quadrupole moment and its abundance in naturally occurring xenon is sufficiently high (26.24%) to make precise measurements with a reasonable signal-to-noise ratio. As indicated by the range of chemical shifts found for xenon compounds (over 5000 ppm, compared to 10–20 ppm for ^{1}H and 600 ppm for ^{19}F), the density dependence of the Xe chemical shift in mixtures of gases is expected to be much greater than the observed density dependence of proton chemical shifts (as much as 0.006 ppm/amagat) and fluorine chemical shifts (as much as 0.018 ppm/amagat).[2] Thus, unlike ^{1}H shifts, ^{129}Xe shifts will not be dominated by bulk susceptibilities. Xenon gas is far from ideal so that one does not have to go to very high partial pressures of xenon in order to have sizeable densities. Furthermore, there is the added advantage that the rare-gas shifts can be referred directly to the gas extrapolated to zero pressure, for which the paramagnetic contribution to shielding is known: $\sigma^{(2)}$ isolated atom $=0$.

The ^{129}Xe shifts in pure gaseous, liquid, and solid xenon were measured by Carr and co-workers and by Norberg and co-workers using broad-line NMR.[3,4] In the pure gas Streever and Carr found a value of σ_1 equal to -0.43 ppm/amagat or -9600 ppm/mol cc^{-1}.[5] Except for the effect of some oxygen impurity in the xenon samples studied by Carr *et al.*, medium effects in mixtures of Xe and other gases have not been previously studied by NMR.

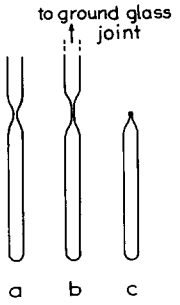

FIG. 1. Typical sample tube (a) after annealing and calibrating, (b) prior to introduction of the sample, (c) final tube containing the sample.

EXPERIMENTAL

Individual sample tubes containing gas mixtures at known densities were prepared. Measurements were carried out in Varian DP-60 and HA-100 spectrometers.

Sample Preparation

We desired to prepare samples at pressures up to about 200 atm. For safety's sake and protection of the spectrometer insert it is desirable to minimize the sample volume. The sample tubes used in most of our work had a volume of about 0.08 ml. The few explosions which we had (because of poor seals) were quite innocuous. The same could definitely not be said for sample volumes greater than about 0.3 ml containing 150 amagats of Xe.

The sample tubes were of borosilicate tubing, 3.9-mm o.d., 1.2-mm i.d., and about 5 cm long. The tubes were prepared as in Fig. 1(a) with a constriction for calibration. After annealing to remove strain the tube volumes were individually calibrated with mercury. They were then sealed to ground-glass joints and the constriction in the sample tube was pulled out to a very small diameter [Fig. 1(b)]. After the sample was introduced the tube could then be sealed off such that the strained area supporting high pressure was minimized [Fig. 1(c)]. We found that the volume of these tubes could be measured accurately to within about 0.0005 ml. This causes an error in the density of less than 1 amagat at 100 amagat.

These small tubes fit nicely into standard 5-mm thin-walled NMR sample tubes. For gases other than Xe convenient external referencing is possible by placing the liquid reference material in the annular region between the tubes.

These small sample tubes can be confidently used to

pressures as high as 200 atm. Larger tubes (2.2-mm i.d.) could be safely used to only about 50 atm.

The gases were used as obtained (Matheson and Company, reagent grade) with degassing of lower boiling constituents and noncondensibles. For gas mixtures, the two gases were kept separately on a vacuum line under liquid nitrogen. Each gas was separately expanded into a calibrated volume (room temperature and subatmospheric pressure). The pressure was noted and the number of moles obtained by assuming ideality. The calibrated volume containing gas was then opened to the previously evacuated sample tube. The gas was swept out of the calibrated volume using mercury. The final "dead" space above the sample tube constriction is very critical. We maintained this at about 1 ml. If this dead space is much larger, then a significant pressure of the condensed gas can remain (on the order of 10 mm Hg or more). Presumably this is because the surface of the solid being frozen out can be at temperatures much greater than liquid-nitrogen temperature in this nonequilibrium system.

Referencing in the case of xenon gas is a definite problem. We used the method of substitution. The resonance signal for a reference was obtained; then the reference is physically exchanged in the probe by the sample while the field is continuously being swept. After the resonance signal of the sample is obtained it is removed and the reference is again placed in the probe and an audio sideband obtained. The field is being swept continually at all times during these substitutions. By averaging over several spectra (upfield and downfield sweeps) we could obtain chemical shifts with a precision of better than ± 0.5 ppm. This is quite acceptable in the case of xenon because of the large density-dependent shifts encountered (signals occurred over a 100-ppm range). For light nuclei the method of substitution would definitely be unacceptable (for ^{19}F compounds the density-dependent shift is only about 1% of that in ^{129}Xe).

The error involved in density measurement is comparable to that caused by the reference method for pure xenon at 100 amagat. The expected error in the chemical shift for each sample measured is about ± 0.5 ppm or somewhat larger for high density samples or in those cases where the density dependence of the chemical shift is large.

We used ^{129}Xe in natural abundance (26.24%). Because of this, the low sensitivity of ^{129}Xe, the low filling factor (1.2-mm tube diameter), the fact that ^{129}Xe is a gas, and the very long relaxation times for ^{129}Xe, it should be expected that we would have sensitivity problems. The spectrometer was run in dispersion mode so that a higher rf field could be used without saturation problems. For low density pure xenon samples small amounts (about 1 amagat) of O_2 were introduced to decrease T_1. The effect of the O_2 contaminant could easily be corrected for. With these precautions and a carefully tuned spectrometer we obtained observable signals (signal/noise about 2) for xenon at 40 amagat in the 1.2-mm tubes. With larger diameter sample tubes we obtained data at lower densities. All NMR spectra were taken at 25°C.

RESULTS

Pure Xenon

The results obtained for pure xenon at 25°C are shown in Fig. 2. If one were to draw a line through the early Streever and Carr data, one would indeed get their reported slope of about -0.43 ppm/amagat. However, the precision of our high-resolution results leaves little doubt that the dependence of ^{129}Xe chemical shift on density is not linear beyond a density of 100 amagats. A least-squares fit of points up to 110 amagats to $\sigma=\sigma_0+\sigma_1\rho$ gives $\sigma_1=-0.548\pm0.004$ ppm/amagat. The experimental points can be fitted to the following expression:

$$\sigma=\sigma_0+\sigma_1\rho+\sigma_2\rho^2+\sigma_3\rho^3,$$

where

$$\sigma_1=-0.548\pm0.004 \text{ ppm/amagat},$$

$$\sigma_2=(-0.169\pm0.02)\times10^{-3} \text{ ppm/amagat}^2,$$

$$\sigma_3=(0.163\pm0.01)\times10^{-5} \text{ ppm/amagat}^3.$$

This is an indication that three or more body collisions become important at high densities. This is not surprising since the highest density of pure xenon gas used here is close to the density of liquid xenon itself. It was not possible to fit all the data within the experimental precision we have demonstrated with just σ_0, σ_1, and σ_2. σ_3 had to be included. The values of σ_2 and σ_3 shown above are reasonable values fit to minimize the square

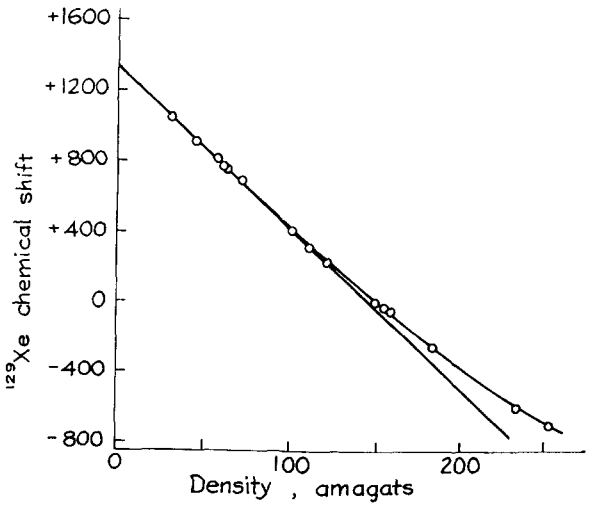

FIG. 2. Density dependence of the ^{129}Xe chemical shift in pure xenon gas.

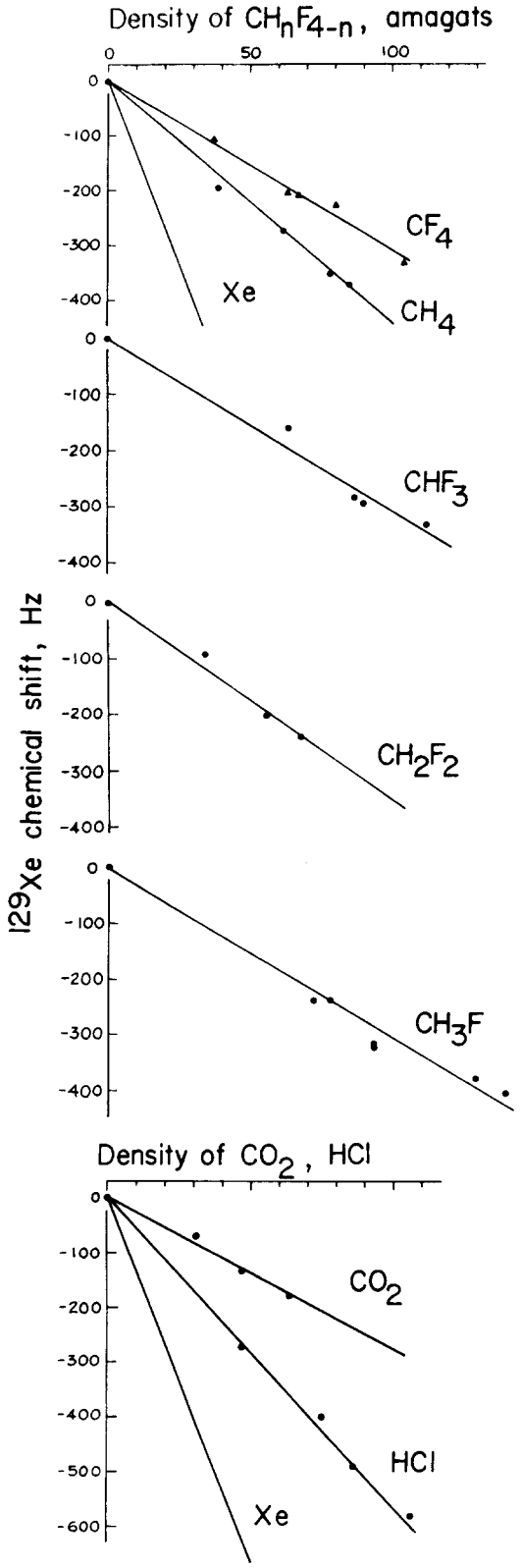

FIG. 3. Density dependence of ^{129}Xe chemical shift in mixtures of xenon with other gases.

TABLE I. Measured values of σ_1(Xe–A).[a]

A	σ_1(Xe–A)
Ar	−3 119±216
CO_2	−3 823±151
CF_4	−4 327±121
CHF_3	−4 287±198
CH_2F_2	−4 965±239
CH_3F	−4 314±170
CH_4	−6 201±125
Kr	−6 070±375
HCl	−7 678±132
Xe	−12 283±90

[a] In parts per million/mole cc^{-1}. These are slopes of lines in Fig. 3 which are least-squares fits to the data points.

of the deviation. However, σ_2 and σ_3 can be chosen somewhat differently and still come close to the minimum square of the deviation. (The minimum square of the deviation is "broad.") Therefore, the values for σ_2 and σ_3 are valid to only about ±10%.

After this work was completed, Kanegsberg, Pass, and Carr[6] reported a similar curvature in their xenon gas data. They fitted their data to linear and quadratic terms, giving a low-density limit at 20°C of −0.61±0.02 ppm/amagat, to be compared with our −0.548±0.004 ppm/amagat at 25°C. Their results are not inconsistent with ours. We have eight data points as opposed to their two in the low-density region up to 110 amagat, and better precision. Moreover, they report a temperature dependence of the curvature.

Mixtures of Xenon with Other Gases

If we assume that only binary collisions are important in mixtures of gases, the chemical shielding of xenon in an A–Xe mixture is given by

$$\sigma = \sigma_0 + \sigma_1(\text{Xe–Xe})\rho_{\text{Xe}} + \sigma_1(\text{Xe–A})\rho_{\text{A}}, \qquad (2)$$

where ρ_{Xe}, ρ_{A} are the densities of Xe and A, respectively. Since σ_1(Xe–Xe) has previously been determined with good precision, σ_1(Xe–A) can be readily determined from data. The results obtained for mixtures of xenon and a second gas, A, are shown in Fig. 3. The plots of Xe chemical shift versus density in these mixtures seems to be reasonably linear. The slopes, σ_1(Xe–A), are shown in Table I.

In the gas mixtures the xenon density varied from 50–150 amagat between samples (mostly about 100 amagat). Although all points for a mixture seem to fit a linear dependence with density within experimental error, we cannot rule out three-body effects in these mixtures, especially in the light of the nonlinear data obtained for pure xenon.

It was anticipated that these results would be a good test of the treatment used by Buckingham *et al.*[1], since

the bulk susceptibility does not dominate (as in ^{1}H) over the desired terms $-A\langle\epsilon_z\rangle-B(\langle\epsilon^2\rangle+\langle F^2\rangle)$. Furthermore, the term linear in electric field is zero so that only *one* parameter (B) is involved. However, the method of Raynes, Buckingham, and Bernstein, which had been quite successful for the analysis of σ_1 values of ^{1}H and ^{19}F nuclei was applied to the experimental slopes for xenon–other-gas mixtures (in Table I) without any success. As shown in Table II, it was not possible to find a common value of the parameter B which could reproduce the values of σ_1 for ^{129}Xe when σ_1 is taken to be

$$\sigma_1(\text{Xe–A})\simeq\tfrac{2}{3}\pi\chi_m(\text{A})-B\langle\epsilon^2\rangle-B\langle F^2\rangle. \quad (3)$$

This indicates that it is not sufficient to include in σ_1(Xe–A) the bulk susceptibility, polar, and van der Waals terms. The terms σ_a and σ_{rep} should be investigated. One should probably also look more closely at the approximation of $-B\langle F^2\rangle$ for the van der Waals contribution. No part of the approximations used in replacing the van der Waals contribution by $-B\langle F^2\rangle$ in the ^{1}H and ^{19}F work makes it any less valid for ^{129}Xe. However, the inadequacy of the $-B\langle F^2\rangle$ term for ^{1}H would not have manifested itself in the studies by Buckingham *et al.* since the ^{1}H shifts were dominated by the bulk susceptibility and the linear electric field term ($-A\langle\epsilon_z\rangle$). In the ^{19}F studies by Bernstein *et al.*, any inadequacy of the $-B\langle F^2\rangle$ terms may not have manifested itself since the $B\langle\epsilon^2\rangle$ contributions though smaller were still of the same order of magnitude as the B$\langle F^2\rangle$ contributions.

It would be desirable to have even an approximate method of calculating B since in this case it can not be obtained by a best fit of the experimental results.

THEORETICAL CONSIDERATIONS

On the Calculation of Parameters A and B

Density dependence of chemical shifts in gases is presently interpreted on the basis of

$$(\partial\sigma/\partial\rho)_T=\sigma_1=-A\langle\epsilon_z\rangle-B\langle\epsilon^2\rangle-B\langle F^2\rangle+\sigma_b,$$

where A and B are empirical "best-fit" parameters and $\langle\epsilon_z\rangle$, $\langle\epsilon^2\rangle$, and $\langle F^2\rangle$ are average values calculated using Stockmayer-type potentials. It would be desirable to have a theoretical calculation of the parameters A and B for the probe molecule particularly in those instances in which the probe molecule or solvent molecule has a sizeable dipole or quadrupole moment.

Since the polar effects of the medium are treated in terms of the instantaneous electric fields produced at the probe molecule by the approach of a solvent molecule, one can find A and B by considering an isolated molecule in a magnetic field H and an external electric field ϵ. The change in the shielding parameter of the probe nucleus due to ϵ will lead to expressions for the parameters A and B.

The Hamiltonian for a molecule in an electric and magnetic field is

$$H_{\text{total}}=H_{0000}+H_\epsilon+H_H+H_\mu+H_{\mu H}+H_{H^2}+H_{\mu^2}, \quad (4)$$

where H_{0000} is the Hamiltonian in the absence of electric and magnetic fields,

$$H_\epsilon=\sum_k -e\mathbf{r}_k\cdot\boldsymbol{\varepsilon}+\sum_N Ze\mathbf{r}_N\cdot\boldsymbol{\varepsilon},$$

$$H_H=(e/2mc)\sum_k \mathbf{H}_0\cdot\mathbf{l}_k,$$

$$H_\mu=(e/mc)\sum_k\sum_N \boldsymbol{\mu}_N\cdot\mathbf{l}_k/r_k^3,$$

$$H_{\mu H}=(e^2/2mc^2)\sum_k\sum_N \boldsymbol{\mu}_N\cdot(r_k^2\hat{I}-\mathbf{r}_k\mathbf{r}_k)\cdot\mathbf{H}_0/r_k^3,$$

$$H_{H^2}=(e^2/8mc^2)\sum_k \mathbf{H}_0\cdot(r_k^2\hat{I}-\mathbf{r}_k\mathbf{r}_k)\cdot\mathbf{H}_0,$$

$$H_{\mu^2}=(e^2/2mc^2)\sum_k\sum_N\sum_{N'}[(\boldsymbol{\mu}_N\times\mathbf{r}_k)\cdot(\boldsymbol{\mu}_{N'}\times\mathbf{r}_k)/r_k^6]. \quad (5)$$

In the absence of the electric field the shielding tensor occurs in the energy term $\boldsymbol{\mu}\cdot\hat{\sigma}\cdot\mathbf{H}_0$ which is obtained from the $H_{\mu H}$ term in the Hamiltonian (first-order energy) and the cross term between the H_μ and H_H terms (second-order energy), the former being called the "diamagnetic contribution" to σ and the latter the "paramagnetic" contribution to σ.

The *change* in σ due to the presence of an electric field comes from terms containing μ, H, and ϵ (or ϵ^2). These originate from: first-order perturbation—none; second-order perturbation—cross term between H_ϵ and $H_{\mu H}$ leads to the contribution to $\Delta(\sigma_{\text{dia}})$ which is linear in ϵ; third-order perturbation—(a) cross term between H_ϵ, H_ϵ, and $H_{\mu H}$ leads to the contribution to $\Delta(\sigma_{\text{dia}})$ which is quadratic in ϵ, (b) cross term between H_ϵ, H_μ, and H_H leads to the contribution to $\Delta(\sigma_{\text{para}})$ which is linear in ϵ; fourth-order perturbation—cross term H_ϵ, H_ϵ, H_μ, and H_H leads to the contribution to $\Delta(\sigma_{\text{para}})$ which is quadratic in ϵ. We see that the expansion perturbation method to second order will give us only A, and only in those chemical shifts in which changes in the diamagnetic term dominate over changes in the paramagnetic term. However, the latter is known to dominate in nuclei other than hydrogen. Perturbation expansions to third and fourth order become rather unwieldy. Therefore, let us consider the perturbation–variational method.

For conciseness let us use subscripts which indicate powers in ϵ, H, μ, and μH, respectively,

$$H_{\text{total}}=H_{0000}+H_{1000}+H_{0100}+H_{0010}+H_{0001}+H_{0200}+H_{0020}. \quad (6)$$

The corrections to the energy[7] are given by

$$E^{(1)}=\langle 0\mid h\mid 0\rangle,$$

$$E^{(2)}=\langle 0\mid h-E^{(1)}\mid 1\rangle,$$

$$E^{(3)}=\langle 1\mid h-E^{(1)}\mid 1\rangle,$$

$$E^{(4)}=\langle 1\mid h-E^{(1)}\mid 2\rangle,\ -\tfrac{1}{2}E^{(2)}\langle 1\mid 1\rangle. \quad (7)$$

TABLE II. Comparison of empirical values of B for ^{129}Xe in various solvent gases, obtained by the method of Raynes, Buckingham, and Bernstein.[a]

Solvent molecule	σ_1 observed	σ_b $(2\pi/3)\chi$	$\sigma_1-\sigma_b$	$\langle\epsilon^2\rangle$[b] 10^{12} (statvolts/cm)^2	$\langle F^2\rangle$[b] 10^{12} (statvolts/cm)^2	B(empirical) $=-(\sigma_1-\sigma_b)/(\langle\epsilon^2\rangle+\langle F^2\rangle)$ 10^{18} (statvolts/cm)$^{-2}$
Ar	−3 119.	−39.	−3 080.	0	8.061	382.
CO_2	−3 823.	−44.	−3 779.	0.0705	9.087	413.
CF_4	−4 327.	−65.	−4 262.	0	11.560	369.
CHF_3	−4 287.	−60.	−4 227.	0.3087	10.976	375.
CH_2F_2	−4 965.	−52.	−4 913.	0.5218	11.912	395.
CH_3F	−4 314.	−44.	−4 270.	0.5074	12.937	318.
CH_4	−6 201.	−36.	−6 165.	0	10.415	592.
Kr	−6 070.	−61.	−6 009.	0	11.876	506.
HCl	−7 678.	−46.	−7 632.	0.1753	12.421	606.
Xe	−12 283.	−95.	−12 188.	0	14.557	837.

[a] Molecular parameters were taken from Ref. 1, except for CH_2F_2 and CH_3F. For these two molecules, χ_m was estimated from Pascal's constants; μ is from C. H. Townes and A. L. Schawlow, *Microwave Spectroscopy* (McGraw-Hill, New York, 1955); α, ϵ, and r_0 are from G. A. Miller and R. E. Bernstein, J. Phys. Chem. **63**, 710 (1959). I was estimated from values for the other fluoromethanes and θ was estimated to be $\pm 1\times10^{-26}$ esu.

[b] Calculated according to the equations in Ref. 1, using integrals $H_6(y)$ and $H_8(y)$ obtained by interpolation from tables given by A. D. Buckingham and J. A. Pople, Trans. Faraday Soc. **51**, 1173 (1955).

Since we are not interested in terms nonlinear in μ and H, we can limit h to

$$h=H_{1000}+H_{0100}+H_{0010}+H_{0001}.$$

The pertinent correction terms in the wavefunction, $|1\rangle$ and $|2\rangle$, are

$$|1\rangle=\psi_{1000}+\psi_{0100}+\psi_{0010}+\psi_{0001}, \tag{8}$$

$$|2\rangle=\psi_{1100}+\psi_{1010}+\psi_{2000}+\psi_{0002}+\psi_{0110}+\psi_{1001}+\psi_{0101}+\psi_{0011}, \tag{9}$$

where ψ's are solutions to differential equations of the type

$$(H_{0000}-E^{(0)})\psi_{1000}-H_{1000}\psi_0=E_{1000}\psi_0, \tag{10}$$

$$(H_{0000}-E^{(0)})\psi_{1100}+(H_{1000}-E_{1000})\psi_{1000}+(H_{0100}-E_{0100})\psi_{0100}=E_{1100}\psi_0. \tag{11}$$

The energies we are interested in are E_{1001} [the term in $\Delta(\sigma_{\rm dia})$ which is linear in ϵ], E_{2001} [the term in $\Delta(\sigma_{\rm dia})$ which is quadratic in ϵ], E_{1110} [the term in $\Delta(\sigma_{\rm para})$ which is linear in ϵ], and E_{2110} [the term in $\Delta(\sigma_{\rm para})$ which is quadratic in ϵ]. Among all the terms which arise in $E^{(2)}$, $E^{(3)}$, and $E^{(4)}$, we need to pick out only the matrix elements which give rise to the above energies. Thus,

$$E_{1001}=\langle 0\,|\,H_{1000}-E_{1000}\,|\,0001\rangle+\langle 0\,|\,H_{0001}-E_{0001}\,|\,1000\rangle,^{8} \tag{12}$$

$$E_{2001}=\langle 1000\,|\,H_{0001}-E_{0001}\,|\,1000\rangle+\langle 1000\,|\,H_{1000}-E_{1000}\,|\,0001\rangle+\text{c.c.}, \tag{13}$$

$$E_{1110}=\langle 1000\,|\,H_{0100}-E_{0100}\,|\,0010\rangle+\text{c.c.}+\langle 1000\,|\,H_{0010}-E_{0010}\,|\,0100\rangle+\text{c.c.}+\langle 1010\,|\,H_{1000}-E_{1000}\,|\,0100\rangle+\text{c.c.}, \tag{14}$$

$$E_{2110}=\langle 1000\,|\,H_{1000}-E_{1000}\,|\,0110\rangle+\langle 1000\,|\,H_{0100}-E_{0100}\,|\,1010\rangle+\langle 1000\,|\,H_{0010}-E_{0010}\,|\,1100\rangle+\langle 0100\,|\,H_{1000}-E_{1000}\,|\,1010\rangle+\langle 0100\,|\,H_{0010}-E_{0010}\,|\,2000\rangle+\langle 0010\,|\,H_{1000}-E_{1000}\,|\,1100\rangle+\langle 0010\,|\,H_{0100}-E_{0100}\,|\,2000\rangle-\tfrac{1}{2}[E_{0110}\langle 1000\,|\,1000\rangle+E_{1010}(\langle 1000\,|\,0100\rangle+\text{c.c.})+E_{1100}(\langle 1000\,|\,0010\rangle+\text{c.c.})+E_{2000}(\langle 0100\,|\,0010\rangle+\text{c.c.})]. \tag{15}$$

The differential equations such as Eqs. (10) and (11) have to be solved for the corrections to the wavefunction and energy, the above matrix elements calculated, and from these energies, the values of A and B may be calculated:

$$\Delta\sigma=(E_{1001}+E_{1110}+E_{2001}+E_{2110})/\mu_N H_0=-A\epsilon-B\epsilon^2,$$

$$A=-(E_{1001}+E_{1110})/\mu_N H_0\epsilon,$$

$$B=-(E_{2001}+E_{2110})/\mu_N H_0\epsilon^2. \tag{16}$$

Calculations of this type remain to be done even for very simple systems (except H atom[9]). An approximate calculation has been done by Musher[10] for A in C–H bonds when only the diamagnetic term in ^{1}H is important. For an H atom or for a hydrogen atom in a molecule, the major contribution to the change in shielding due to the electric field is that due to E_{1001} which is relatively easy to calculate. However, for Xe atom, $A=0$ and the major contribution to B is that due to E_{2110}, which is not at all trivial to evaluate since it involves second-order corrections to the wavefunction.

TABLE III. Calculated values of B for hydrogen and the rare-gas atoms.

Probe	$\alpha^a\times10^{24}$ cm^3	$\Delta E\times10^{12}$ ergs[b] $np\rightarrow(n+1)s$	$np\rightarrow(n+1)p$	$np\rightarrow nd$	$\langle a_0^3/r^3\rangle_{np}$[c]	$\langle a_0^3/r^3\rangle_{(n+1)p}$	$\langle a_0^3/r^3\rangle_{nd}$	$B\times10^{18}$ (statvolts/cm)$^{-2}$ $np\rightarrow(n+1)s$	$np\rightarrow(n+1)p$	$np\rightarrow(nd)$	Average
H	0.666	16.34	16.34			0.042		0.35			0.35
He	0.216	31.72	33.64			0.106		0.0674	0.083		0.075
Ne	0.398	26.59	29.48		11.1	6.8		4.83	6.35		5.6
Ar	1.63	18.42	20.66	22.11	10.8	4.1	1.5	40.2	44.1	39.5	41.3
Kr	2.48	15.86	18.10	19.22	19.1	1.3	0.6	145.8	119.5	108.8	124.7
Xe	4.01	13.30	15.38	15.86	22.3	1.2	1.0	391.6	308.2	312.0	337.3

[a] *Landolt-Bornstein Zahlenwerte und Funktionen* (Springer, Berlin, 1950), Vol. 1, Part 1, p. 401.
[b] C. Moore, Natl. Bur. Std. (U.S.) Circ. **467** (1958). Except for H and He, in which ΔE refers to the $1s\rightarrow2s$ or $2p$ excitation, n stands for the quantum number of the outermost electrons.
[c] Estimated according to R. G. Barnes and W. V. Smith, Phys. Rev. **93**, 95 (1954).

This term is presently being investigated. Here we consider an approximate calculation of B.

Approximation Calculation of B for a Monatomic Molecule Probe

The approach here is to calculate the change in the system due to the application of the electric field, then calculate the change in chemical shielding brought about by this.

For an atomic system perturbed by an electric field, second-order perturbation theory gives the correction to the energy:

$$E^{(2)}=E_\epsilon=-\sum_n\left[\langle 0\mid h\mid n\rangle\langle n\mid h\mid 0\rangle/(E_n-E_0)\right], \quad (17)$$

where $h=\sum_k -e\mathbf{r}_k\cdot\boldsymbol{\epsilon}$ is the perturbing Hamiltonian. Let us write the energy correction E_ϵ in terms of contributions of various excited states n,

$$E_\epsilon=\sum_n e_n, \quad \text{where} \quad e_n=-\langle 0\mid h\mid n\rangle^2/(E_n-E_0). \quad (18)$$

The wavefunction correct to first order is given by

$$\psi^{(1)}=\psi^{(0)}+\sum_n \lambda_n\psi_n,$$

where

$$\lambda_n=-\langle n\mid h\mid 0\rangle/(E_n-E_0),$$

$\psi^{(0)}$ is the ground-state Slater determinant, and the ψ_n are Slater determinants in which higher atomic orbitals are used. We see that

$$e_n/(E_n-E_0)=-\langle 0\mid h\mid n\rangle^2/(E_n-E_0)^2. \quad (19)$$

Thus,

$$\lambda_n^2=\mid e_n/(E_n-E_0)\mid. \quad (20)$$

If we can use an average excitation energy ΔE,

$$\lambda^2\equiv\sum_n\lambda_n^2\simeq(\Delta E)^{-1}\sum_n\mid e_n\mid=(\Delta E)^{-1}\mid E_\epsilon\mid.$$

But for an atom, $E_\epsilon=-\frac{1}{2}\alpha\epsilon^2$, where α is the electric polarizability of the atom. Thus,

$$\lambda^2\simeq\tfrac{1}{2}(\alpha\epsilon^2/\Delta E). \quad (21)$$

This corresponds to the total fraction of electrons excited from the ground configuration $\psi^{(0)}$ to higher energy configurations ψ_n.

This change in the atom due to the electric field ϵ gives rise to a change in the chemical shielding, $\Delta\sigma$, as a function of λ^2. This change in chemical shielding can be considered in terms of the changes in the diamagnetic and paramagnetic contributions to shielding.

As has been pointed out in earlier work on chemical shift calculations, with origin centered on the nucleus in question, the $\sigma^{(2)}$ contribution lends itself to calculation in terms of populations, $p_{\mu\nu}$, of p and d orbitals of the atom in question.[11,12] The paramagnetic shielding can be calculated in terms of λ^2 using the formulation

developed in Ref. 12:

$$\sigma^{(2)} = -(2e^2\hbar^2/3\Delta m^2c^2)\{\langle 1/r^3\rangle_{5p}[(p_{xx}+p_{yy}+p_{zz}) - \tfrac{1}{2}(p_{zz}p_{yy}+p_{xx}p_{yy}+p_{xx}p_{zz}+\tfrac{1}{2}(p_{yz}p_{zy}+p_{xy}p_{yx} + p_{xz}p_{zx})] + \langle 1/r^3\rangle_{5d}[3(p_{z^2,z^2}+p_{xz,xz}+p_{xy,xy} + p_{x^2-y^2,x^2-y^2}+p_{yz,yz}) - \tfrac{3}{2}(\tfrac{4}{3}p_{x^2-y^2,x^2-y^2}p_{xy,xy} + p_{z^2,z^2}p_{xz,xz}+p_{z^2,z^2}p_{yz,yz}) - \tfrac{1}{2}(p_{x^2-y^2,x^2-y^2}p_{xz,xz} + p_{x^2-y^2,x^2-y^2}p_{yz,yz}+p_{xy,xy}p_{yz,yz}+p_{xy,xy}p_{xz,xz} + p_{xz,xz}p_{yz,yz}) + \text{terms involving } p_{xy,yz} \text{ etc.}]\}, \quad (22)$$

where p_{xx}, p_{yy}, and p_{zz} are orbital populations of the $5p_x$, $5p_y$, and $5p_z$ orbitals, respectively. If we envisage a promotion of λ^2 electrons from $5p_z$ to $(5d_{xy}+5d_{x^2-y^2})/\sqrt{2}$,[13]

$$p_{xx}=p_{yy}=2, \qquad p_{zz}=2-\lambda^2,$$

$$p_{z^2,z^2}=p_{xz,xz}=p_{yz,yz}=0,$$

and

$$p_{xy,xy}=p_{x^2-y^2,x^2-y^2}=\tfrac{1}{2}\lambda^2.$$

All cross terms such as p_{xy} or $p_{xz,yz}$ are equal to zero.

TABLE IV. Values of the constants $A\times10^{12}$ (statvolts/cm)$^{-1}$ and $B\times10^{18}$ (statvolts/cm)$^{-2}$.

Nucleus	Probe molecule	Empirical A	Empirical B	Calculated A	Calculated B	Ref.
^{1}H	H atom			0	0.35	a
	H atom			0	0.20	b
	H atom			0	0.74	c
	H_2			1.45		d
	CH bond			2.	1	e
	CH bond			2.9		f
	CHF_3	2.9	0.74			g
	CH_3Cl	8.	0.30			h
	$(CH_3)_2O$	16.	1.00			h
	H_2S	26.	0.65			h
	HCl	40.	0.38			i
	HBr	65.	1.60			h
^{19}F	CHF_3	−9.9	15.1			j
	CF_4		16.4			j
	SF_6		29.5			j
	SiF_4		43.5			j
He	He			0	0.075	a
Ne	Ne			0	5.6	a
Ar	Ar			0	41.3	a
Kr	Kr			0	124.7	a
^{129}Xe	Xe			0	337.3	a

[a] This work.
[b] T. W. Marshall and J. A. Pople, Mol. Phys. **3**, 339 (1960).
[c] T. W. Marshall and J. A. Pople, Mol. Phys. **1**, 199 (1958).
[d] J. I. Musher, Advan. Mag. Res. **2**, 177 (1966).
[e] A. D. Buckingham, Can. J. Chem. **38**, 300 (1960).
[f] J. I. Musher, J. Chem. Phys. **37**, 34 (1962).
[g] L. Petrakis and H. J. Bernstein, J. Chem. Phys. **37**, 2731 (1962).
[h] G. Widenlocher and E. Dayan, Compt. Rend. **260**, 6856 (1965).
[i] W. E. Raynes, A. D. Buckingham, and H. J. Bernstein, J. Chem. Phys. **36**, 3481 (1962).
[j] L. Petrakis and H. J. Bernstein, J. Chem. Phys. **38**, 1562 (1963).

TABLE V. Comparison of observed σ_1(Xe–A) with the values of the calculated contributions to σ_1.

A	Calculated σ_b	Calculated σ_ϵ	Calculated σ_W	Calculated σ_1(Xe–A)[a]	Observed σ_1(Xe–A)
Ar	−39.	0.	−2719.	−3516.	3 119.
CO_2	−44.	−24.	−3065.	−4385.	3 823.
CF_4	−65.	0.	−3899.	−5121.	4 327.
CHF_3	−60.	−104.	−3702.	−5263.	4 287.
CH_2F_2	−52.	−176.	−4018.	−5832.	4 965.
CH_3F	−45.	−171.	−4364.	−6054.	4 314.
CH_4	−36.	0.	−3513.	−4481.	6 201.
Kr	−61.	0.	−4006.	−5020.	6 070.
HCl	−46.	−59.	−4190.	−5354.	7 678.
Xe	−95.	0.	−4910.	−6266.	12 283.

[a] This includes the contribution σ_{rep} which is shown in Table VI.

These values when substituted into $\sigma_{Xe}^{(2)}$ give

$$\Delta\sigma_{Xe}^{(2)}(5p\rightarrow5d) = [-2e^2\hbar^2/3\Delta E(5p\rightarrow5d)m^2c^2] \times[\langle 1/r^3\rangle_{5p}\lambda^2+\langle 1/r^3\rangle_{5d}(3\lambda^2-\tfrac{1}{2}\lambda^4)]. \quad (23)$$

Similarly,

$$\Delta\sigma_{Xe}^{(2)}(5p\rightarrow6s) = [-2e^2\hbar^2/3\Delta E(5p\rightarrow6s)m^2c^2]\langle 1/r^3\rangle_{5p}\lambda^2, \quad (24)$$

$$\Delta\sigma_{Xe}^{(2)}(5p\rightarrow6p) = [-2e^2\hbar^2/3\Delta E(5p\rightarrow6p)m^2c^2] \times[\langle 1/r^3\rangle_{5p}\lambda^2+\langle 1/r^3\rangle_{6p}\lambda^2]. \quad (25)$$

Generalization of the above equations for $(np\rightarrow nd)$, $[np\rightarrow(n+1)s]$, and $[np\rightarrow(n+1)p]$ excitations for any rare-gas atom is trivial.

The diamagnetic contribution to chemical shielding, σ_{dia} or $\sigma^{(1)}$, is itself quite large for atoms of high Z,[14] whereas σ_{para} or $\sigma^{(2)}$ is zero for the spherically symmetric atom in the absence of an electric field. However, *changes* in $\sigma^{(1)}$ for atoms of high Z are negligible in comparison to changes in $\sigma^{(2)}$, as has been shown previously.[12] For example, the change in $\sigma^{(1)}$ and $\sigma^{(2)}$ due to excitation of a fraction, λ^2, of electrons from $5p$ to $6s$ in Xe is given by

$$\Delta\sigma_{Xe}^{(1)} = \lambda^2(e^2/3mc^2)(-\langle 5p \mid 1/r \mid 5p\rangle+\langle 6s \mid 1/r \mid 6s\rangle).$$

The first term is $\sim-4.2\lambda^2$ ppm[14], and the second is estimated to be about $+2\lambda^2$ ppm. Thus, $\Delta\sigma_{Xe}^{(1)}\simeq-2.\lambda^2$ ppm. On the other hand,

$$\Delta\sigma_{Xe}^{(2)}(5p\rightarrow6s) = -\frac{2e^2\hbar^2\langle 1/r^3\rangle_{5p}\lambda^2}{3\Delta E(5p\rightarrow6s)m^2c^2} \simeq -2590\lambda^2 \text{ ppm}.$$

Therefore, for Xe, $\Delta\sigma^{(1)}$ is clearly negligible compared to $\Delta\sigma^{(2)}$. For a helium atom, $\Delta\sigma^{(1)}$ is not negligible.

The results of calculations of $\Delta\sigma$ for rare-gas atoms in an electric field ϵ are shown in Table III. Empirical values of $\langle 1/r^3\rangle$ were evaluated from spin–orbit splitting

parameters obtained from atomic spectra. Equation (21),

$$\lambda^2 \simeq \tfrac{1}{2}(\alpha/\Delta E)\epsilon^2, \qquad (21)$$

is substituted into the above expressions for $\Delta\sigma$. Three excitations were considered: $np \rightarrow (n+1)s$, $np \rightarrow (n+1)p$, and $np \rightarrow nd$, and $\Delta\sigma^{(2)}$ were calculated according to Eqs. (23)–(25). For H and He, $\Delta\sigma^{(1)}$ was also calculated. The coefficient of ϵ^2, which is $-B$, is obtained as an average over these three. The values of B calculated here are compared with values for other systems in Table IV. The calculated values of B appear to be of the right order of magnitude, and the value for ^{129}Xe, 337.3×10^{-18} (statvolts/cm)$^{-2}$, is not very different from the values of B which could have been extracted from experiment from some of the Xe–other gas mixtures (Table II). Calculated values of the different contributions to σ_1 using this value of B are shown in Table V.

The successful analysis by Bernstein *et al.* of the values of σ_1 in ^{1}H probes (in which σ_1 is dominated by bulk susceptibility and polar terms) and in ^{19}F probes (in which σ_1 is dominated by the quadratic polar and the van der Waals terms) showed that $-A\langle\epsilon_z\rangle - B\langle\epsilon^2\rangle$ and $-B\langle F^2\rangle$ are probably adequate expressions for the polar and van der Waals contributions to σ_1. However, it is clear from Tables II and V, that these terms alone do not explain the results obtained here. Therefore let us consider the terms due to anisotropy (σ_a) and repulsive interactions (σ_{rep}).

On the Anisotropy Contribution to σ_1

The neighbor anisotropy term, σ_a, which was found to be negligible in the cases previously studied, is also found to be negligible in the case of ^{129}Xe. This contribution is given by[15]

$$\sigma_a \simeq -\tfrac{1}{3}(\chi_{||}-\chi_\perp)(3\cos^2\theta_2-1)R^{-3},$$

where $\chi_{||}$ and $\chi_\perp$ are the molecular susceptibilities of the solvent molecule along and perpendicular to its molecular axis, and θ_2 is the angle which this axis makes with R. In those cases in which the probe molecule and the solvent molecule both have dipole moments, $\langle(3\cos^2\theta_2-1)R^{-3}\rangle$ is nonzero, the collisions are nonisotropic due to the interactions of the dipoles. However, xenon has no dipole moment, so that, to a first approximation, σ_a is zero. In pure xenon gas, an estimate of σ_a of an Xe atom can be made from a consideration of the chemical shielding of a second Xe atom contributed by the first. An estimate of this shielding can be made as suggested by Pople,[16] and as was done previously for Xe in the xenon fluorides.[17] The shielding due to the neighbor atom is approximately given by

$$\eta/3\langle 1/r^3\rangle_{5p}R^3,$$

where η is the anisotropy in the chemical shielding of the neighbor atom. The hole in the $5p$ gives rise to the major portion of the anisotropy,

$$\eta \simeq -\lambda^2\langle 1/r^3\rangle_{5p}(-e^2\hbar^2/\Delta E m^2c^2).$$

Thus,

$$\sigma_a \simeq +(\lambda^2/R^3)(e^2\hbar^2/3\Delta E m^2c^2).$$

This is about $0.5\lambda^2$ ppm at $R=4.07$ Å (the minimum of the Xe Lennard-Jones potential), even smaller than the change in the diamagnetic shielding, and is probably negligible even for mixtures of xenon and other gases.

On the Repulsive Contribution to σ_1

The repulsive contribution to σ_1 for Xe probe in Xe gas was calculated by Adrian[18] to explain the earlier results of Carr and co-workers. His calculation led to a σ_1 which he reports as almost exclusively a repulsive contribution of -0.28 ppm/amagat.[19]

The repulsive contribution to σ_1 can be estimated by a method similar to that used in the interpretation of hyperfine shifts.[20] The hyperfine shift was taken to be proportional to the ratio of the interaction energy between the atoms and the average excitation energy of the alkali atom. Here the repulsive contribution to the shift is assumed to be proportional to the ratio of the repulsive part of the potential to the average excitation energy. If we assume that a fraction λ_{rep}^2 analogous to the λ^2 in the calculation of B is given by

$$\lambda_{\text{rep}}^2 = \tfrac{1}{2}V_{\text{rep}}/\Delta E$$

for like atoms (a similar form for unlike atoms, with a weighting factor f instead of $\frac{1}{2}$), then the repulsive contribution to the Xe chemical shift due to Xe–A collisions is given by

$$\Delta\sigma_{\text{Xe}}^{(2)}(\text{rep}) \simeq (2e^2\hbar^2/3\Delta E m^2c^2)\langle 1/r^3\rangle_{5p} f \times[4\pi N r_0^3 \epsilon H_{12}(y)/3\Delta E y^4].$$

Here $y=2(\epsilon/kT)^{1/2}$ as in Ref. 1, and the integrals $H_{12}(y)$ are calculated by interpolation of the Buckingham–Pople tables.[21] If A is a polyatomic molecule, a central field potential for Xe–A is probably no longer adequate (see next section). The calculated values for σ_{rep} are shown in Table VI.

TABLE VI. Calculated repulsive contribution to σ_1 for Xe probe in other gases.[a]

Ar	−757.6
CO_2	−1252.2
CF_4	−1156.6
CHF_3	−1397.4
CH_2F_2	−1586.0
CH_3F	−1473.8
CH_4	−932.1
Kr	−953.1
HCl	−1059.2
Xe	−1260.9

[a] In parts per million/mole cc^{-1}.

As we can see in Table V, the approximate σ_{rep} values do not greatly improve agreement with experiment. The disagreement is the worst in the cases of greatest slope. A better calculation of σ_1 is required. Perhaps the many-body techniques applied by Das and his group to the hyperfine pressure shift can be used, with some approximations owing to the large number of electrons in Xe.

The Relative Magnitudes of σ_1 (Xe–CH_nF_{4-n})

The results of CH_4–Xe and CF_4–Xe mixtures are contrary to what one might predict for an interaction which is dependent on polarizability. σ_1 decreases monotonically in the series Xe, Kr, Ar (Fig. 3) as does the polarizability. Yet σ_1 for CH_4 and CF_4 are in the reverse order, σ_1 being larger for CH_4–Xe than for CF_4–Xe mixtures. However, this is not peculiar to our xenon results. $(\sigma_1-\sigma_b)$ has also been found to be of larger magnitude for CH_4 than CF_4 gas in all other instances where data were taken in both gases[2] (see Table VII). The calculated values in all these instances were in the reverse order. However, this was not particularly noted at the time since the differences between observed and calculated values were not much more than in other gases studied.

In the results for the fluoromethanes in this work (see Table I), as well as the results for ^{19}F in CF_4 and CHF_3, in CH_nF_{4-n} solvents, the relative magnitudes of σ_1 in CH_nF_{4-n} solvents is opposite to that predicted. Of the approximations used in the Raynes, Buckingham, and Bernstein treatment, the weakest one is probably the use of the form $-B\langle F^2\rangle$ for the long-range (van der Waals) interactions. The failure of this treatment in the CH_nF_{4-n} solvents may imply that the weakness of this approximation shows up in these cases. However, we cannot say this with assurance. It may be that we are seeing the inadequacy of the central-field intermolecular potential function used. A larger value of $\sigma_W+\sigma_{rep}$ would be obtained with a deeper potential, since the integral in the ensemble average for σ_W is of the form $\int R^{-6}\exp[-V(R)/kT]R^2dR$ and that for the repulsive contribution can be approximated by $\int R^{-12}\exp[-V(R)/kT]R^2dR$. Thus, it appears from our values of σ_1(Xe–CH_4) and σ_1(Xe–CF_4) that the Xe–CH_4 potential is actually deeper than the Xe–CF_4 potential.

TABLE VII. Comparison of $[\sigma_1(\text{observed})-\sigma_b]$[a] in solvents CH_4 and CF_4.[b]

Probe	Solvent gas CH_4	Solvent gas CF_4
^{19}F, CF_4	−136	−91
^{19}F, CHF_3	−140	−60
^{1}H, CHF_3	−10	−9
^{129}Xe, Xe	−6165	−4262

[a] In parts per million/mole cc^{-1}.
[b] All but Xe are taken from L. Petrakis and H. J. Bernstein, J. Chem. Phys. 37, 2731 (1962); 38, 1562 (1963).

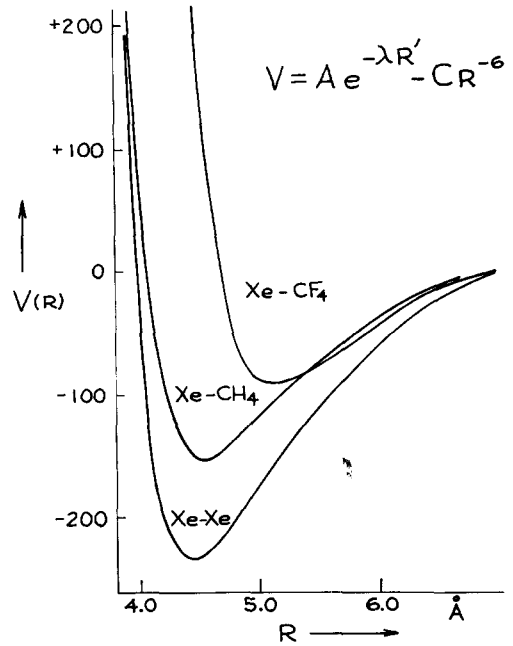

FIG. 4. Calculated exp-6 potentials for Xe–CH_4 and Xe–CF_4 interactions, compared with Xe–Xe potential.

The Lennard-Jones potential places the attractive as well as the repulsive centers at the center of mass of the molecule. For the long-range (attractive) part, this is probably correct, but for the short-range interactions, the repulsive centers are more reasonably placed at the peripheral atoms since at close range the Xe electrons interact primarily with the H or F valence electrons. If we construct such a potential function from known potential function parameters and approximate combining rules, we could at least see whether placing the repulsive centers at the peripheral atoms does lead to a potential function capable of explaining the relative magnitudes of σ_1(Xe–CH_nF_{4-n}). Such potential functions for Xe–CH_4 and Xe–CF_4 were constructed from known potential function parameters and approximate combining rules. The parameters used are shown in Table VIII. A simple two-center potential form is used,

$$V=A\exp(-\lambda r')-C/r^6,$$

in which the $-C/r^6$ (attractive) part is centered on the C and Xe atoms and the $A\exp(-\lambda r')$ part is centered on the H (or F) and Xe atoms.[22] The latter short-range part of the potential should be characteristic of Xe interacting with H (or F) in the molecular environment, and is approximated to be the same as Xe interacting with He (or Ne) at these positions. The angular structure of CH_4 and CF_4 is neglected, only the linear configuration (C–H···Xe) is considered. The potential functions are drawn in Fig. 4 and compared with that

TABLE VIII. Parameters of the exp-6 potential used in Xe–CH_4 and Xe–CF_4 interactions.[a]

	Xe	CH_4	CF_4
C–H (C–F) bond length		1.093 Å[b]	1.323 Å[c]
α (cm^3)	4.0×10^{-24} [d]	2.6×10^{-24} [d]	2.9×10^{-24} [e]
C/k (Xe–A) (°K)	3.35×10^{6} [f]	2.18×10^{6} [g]	2.43×10^{6} [g]
A/k (Xe–A) (°K)	8.63×10^{7} [f]	1.34×10^{7} [h]	6.73×10^{7} [h]
λ (Xe–A) ($Å^{-1}$)	2.92 [f]	3.44 [h]	3.76 [h]

[a] The combining rules for unlike atoms which were used were: $A_{12}=(A_{11}A_{22})^{1/2}$, $\lambda_{12}=\frac{1}{2}(\lambda_{11}+\lambda_{22})$, $C_{12}=(C_{11}C_{22})^{1/2}$.

[b] G. Herzberg, *Molecular Spectra and Molecular Structure, II. Infrared and Raman Spectra of Polyatomic Molecules* (Van Nostrand, Princeton, N. J., 1960), p. 182.

[c] D. Peters, J. Chem. Phys. **38,** 561 (1963).

[d] *Landolt-Bornstein Zahlenwerte und Funktionen* (Springer, Berlin, 1951).

[e] L. Petrakis and H. J. Bernstein, J. Chem. Phys. **38,** 1562 (1963).

[f] Calculated from values for exp-6 potential given by E. A. Mason, J. Chem. Phys. **23,** 49 (1954). $r_m=4.45$ Å; $\lambda r_m=13.0$, $\epsilon/k=231.2$°K.

[g] Calculated from the usual combining rules and the first-order relation between α and C, J. O. Hirschfelder, C. F. Curtiss, and R. B. Bird, *Molecular Theory of Gases and Liquids* (Wiley, New York, 1964), pp. 964ff.

[h] Calculated from the usual combining rules for interaction between Xe–He and Xe–Ne, parameters from Ref. f: for He, $r_m=3.135$ Å, $\lambda r_m=12.4$, $\epsilon/k=9.16$°K; for Ne, $r_m=3.147$ Å, $\lambda r_m=14.5$, $\epsilon/k=38.0$°K.

of Xe–Xe. Clearly, even though the polarizability α is larger for CF_4 than for CH_4, the potential well constructed for CH_4 is deeper. This dramatic difference is due to the much more rapid falloff of the repulsive interaction with xenon–carbon distance for Xe–CH_4 when compared to Xe–CF_4. This rapid falloff is due to shorter CH than CF distance and small A_{12} for Xe–CH_4 compared to Xe–CF_4. According to this crude analysis, the potential function for mixed gases, in which one of the molecules has peripheral hydrogen atoms, should be characterized by an especially deep potential well with a "hard" repulsive part.

We have shown that it may be possible to explain the density dependence of Xe–CH_4 and Xe–CF_4 mixtures on the basis of quite different potential functions rather than on the basis of unusual collisional effects on the chemical shielding. A related observation which could be explained by potential functions of this type is the solvent shift in $J(^{29}Si–F)$ in SiF_4. The coupling constant is found to be shifted by solvents, the shifts increasing monotonically with increasing n in a series of related solvents of formula CX_nF_{4-n} or SiX_nF_{4-n}.[23] These shifts are additive in terms of a characteristic shift per substituent atom (or group) on the carbon or silicon.[24] These characteristic shifts per substituent increases in the order

$$Si–F\approx C–F\approx 0<C–H\approx 1.2<Si–Me\approx 1.5<C–CN$$
$$\approx 1.66<C–Cl\approx 2.0<Si–Br\approx 2.5<Si–Et\approx 3.0 \text{ Hz}.$$

Furthermore, the shift in C_6H_6 was much greater than in C_6F_6 (7.98 Hz vs 4.44 Hz, respectively). The order of shifts due to F, Cl, and Br substituent is not altogether surprising. If Xe–CCl_4 and Xe–CBr_4 approximate potential functions were constructed in the same way as those in Fig. 4, the depths of the potential wells are expected to be in the order Xe–CF_4<Xe–CH_4<Xe–CCl_4<Xe–CBr_4 due to much greater polarizabilities of CCl_4 and CBr_4 compared to CF_4. Thus, the order Si–F≈C–F<C–H<C–Cl<Si–Br could be explained on the basis of the potential functions of SiF_4 with molecules having C–F, C–H, C–Cl, or C–Br groups having well depths in the order indicated. Other solvent shifts of coupling constants such as J_{FF}(vicinal) have also been found to be larger when H's are substituted for F's in the solvent molecule. These were thought to be due to specific F–F interactions. However, in view of the SiF_4 J(Si–F) solvent shifts, the σ_1^{Xe}(Xe–CH_nF_{4-n}), and the σ_1^{F}(CH_nF_{4-n}–CH_mF_{4-m}) given in Table VII, it is likely that the effect is consistent with these others and that all these phenomena are related. At this point it is speculative to explain all these data by means of expected differences in the potential functions. However, Fig. 4 indicates that it is likely that such differences in potential functions exist.

* This research was supported by the U.S. Office of Naval Research and by the National Science Foundation.

[1] W. T. Raynes, A. D. Buckingham, and H. J. Bernstein, J. Chem. Phys. **36,** 3481 (1962); L. Petrakis and H. J. Bernstein, *ibid.* **38,** 1562 (1963); G. Widenlocher, Ann. Phys. (Paris) **1,** 327 (1966).

[2] P. Laszlo, Progr. Nucl. Magnetic Resonance Spectry. **3,** 231 (1967).

[3] R. L. Streever and H. Y. Carr, Phys. Rev. **121,** 20 (1961); E. R. Hunt and H. Y. Carr, *ibid.* **130,** 2302 (1963).

[4] W. M. Yen and R. E. Norberg, Phys. Rev. **131,** 269 (1963). Chemical shifts in liquid and solid xenon have been studied by D. Brinkmann, Phys. Rev. Letters **13,** 187 (1964); W. W. Warren and R. E. Norberg, Phys. Rev. **148,** 402 (1966); D. Brinkmann and H. Y. Carr, *ibid.* **150,** 174 (1966).

[5] One amagat is the density of the gas at standard conditions.

[6] E. Kanegsberg, B. Pass, and H. Y. Carr, Phys. Rev. Letters **23,** 572 (1969).

[7] A. Dalgaron, in *Quantum Theory*, edited by D. R. Bates (Academic, New York, 1961), Vol. 1, p. 171.

[8] This term has been previously discussed by J. I. Musher, Advan. Magnetic Resonance **2,** 177 (1966), for an H atom in an electric field.

[9] T. W. Marshall and J. A. Pople, Mol. Phys. **3,** 339 (1960).

[10] J. I. Musher, J. Chem. Phys. **37,** 34 (1962).

[11] M. Karplus and T. P. Das, J. Chem. Phys. **34,** 1683 (1961).

[12] C. J. Jameson and H. S. Gutowsky, J. Chem. Phys. **40,** 1714 (1964).

[13] It turns out that it is immaterial which of the d orbitals one uses since a different choice leads to only second-order changes (terms of order λ^4).

[14] W. C. Dickinson, Phys. Rev. **80,** 563 (1950).

[15] M. J. Stephen, Mol. Phys. **1,** 223 (1958).

[16] J. A. Pople, Proc. Roy. Soc. (London) **A239,** 541, 550 (1957).

[17] C. J. Jameson and H. S. Gutowsky, J. Chem. Phys. **40,** 2285 (1964).
[18] F. J. Adrian, Phys. Rev. **136,** A980 (1964).
[19] The overlap integral ($S_{\sigma\sigma}+S_{\pi\pi}$) at $R=4.07$ Å was found to be 0.0789, much smaller than Adrian's value of 0.248. This overlap integral was checked by an independent calculation using directly the tabulated $P(\mu x)$ function for Xe and the Monte Carlo method of integration. The result was 0.079, in good agreement with 0.0789.
[20] F. J. Adrian, J. Chem. Phys. **32,** 972 (1960).
[21] A. D. Buckingham and J. A. Pople, Trans. Faraday Soc. **51,** 1173 (1955).
[22] In other words, r is the C–Xe internuclear distance, whereas r' is the H (or F)–Xe internuclear distance.
[23] T. D. Coyle, R. B. Johannesen, F. E. Brinkman, and T. C. Farrar, J. Phys. Chem. **70,** 1682 (1966).
[24] Also noted by W. T. Raynes, Mol. Phys. **15,** 435 (1968).

THE JOURNAL OF CHEMICAL PHYSICS VOLUME 53, NUMBER 6 15 SEPTEMBER 1970

Pure Thermal Diffusion. I. Time-Dependent Phenomenological Theory for Binary Liquids*

FREDERICK H. HORNE AND TERRY G. ANDERSON†
Department of Chemistry, Michigan State University, East Lansing, Michigan 48823
(Received 16 March 1970)

Solutions to the partial differential equations which describe pure thermal diffusion in a binary liquid are obtained by means of perturbation and Fourier transform methods which retain explicitly the temperature and composition dependences of density, heat capacity, and the coefficients of diffusion, thermal diffusion, and thermal conductivity. Inclusion of the effects of time-dependent temperature and center-of-mass velocity gradients during the warming-up period yields unambiguous identification of zero time. Inclusion of the variability of the coefficients makes it possible to evaluate the effects of such variability. The theory provides clear criteria for experimental design. Practical formulas are given for both demixing and remixing experiments.

I. INTRODUCTION

Thermal diffusion, the partial demixing of fluid mixtures due to diffusion fluxes induced by temperature gradients, can be studied in at least four ways.[1] Pure thermal diffusion[1,2] is characterized by a vertical temperature gradient and the absence of forced convective flow, while thermogravitational experiments[1,3] utilize a temperature difference applied horizontally so that the resulting natural convection enhances the diffusive demixing. A flow cell method which combines a vertical temperature difference and forced flow has recently been described.[4] The fourth method[1,5] involves the use of two chambers separated by a porous glass plate or a membrane and provided with stirring devices.

Pure thermal diffusion is conceptually the simplest and, therefore, perhaps the most suitable to a complete description. Previous phenomenological theories of pure thermal diffusion have been obtained by assuming that the coefficients of diffusion, thermal diffusion, and thermal conductivity are constants in any single experiment. There exist, however, common systems for which these transport parameters change appreciably over the temperature ranges ordinarily encountered. Furthermore, time-dependent temperature distributions, convective heat and mass transfer, and the composition dependence of density have previously been neglected. Since exact solutions are not obtainable for the partial differential equations which describe the simultaneous heat and mass transport in a pure thermal diffusion cell, one seeks approximate solutions which are sufficiently complete to describe all experimentally observable phenomena. We obtain such solutions by means of perturbation and Fourier transform methods which retain explicitly the temperature and composition dependences of density, of heat capacity, and of all transport parameters. We also take full account of both convective transport and warming-up effects, and we obtain expressions for the temperature, composition, and center-of-mass velocity as functions of position and time. Of particular significance for application to experiment is our unambiguous definition of zero time.

The classical pure thermal diffusion cell[1,2] is a rectangular parallelepiped bounded above and below by flat, inert metal plates in contact with reservoirs which can be maintained at any desired temperatures. The uniform plate separation, which may be between a fraction of a millimeter and several centimeters, is usually optimized to reduce the time required to reach a steady state without unduly hampering observation. Typically, glass cell walls between the upper and lower metal plates contain the fluid and permit *in situ* measurements of refractive index changes. For other detection methods, such as electrolytic conductance,[1,2d] the lateral walls may be of any suitable material.

After initial equilibration at some uniform temperature, the temperatures of the metal plates are changed in such a way that a negative vertical density gradient is produced in the fluid, i.e., the denser portion of the fluid is closer to the center of the earth.[6] The presence of the temperature gradient induces a diffusion flux which tends to demix the fluid. If the temperature gradient is maintained, eventually a steady state is reached in which the demixing due to thermal diffusion